



Article

A Decision-Tree Approach to Identifying Paddy Rice Lodging with Multiple Pieces of Polarization Information Derived from Sentinel-1

Xuemei Dai ^{1,2,3}, Shuisen Chen ^{2,4,*} , Kai Jia ^{2,4} , Hao Jiang ² , Yishan Sun ², Dan Li ², Qiong Zheng ^{2,5} and Jianxi Huang ⁶

¹ Guangzhou Institute of Geochemistry, Chinese Academy of Sciences, Guangzhou 510640, China

² Guangdong Provincial Key Laboratory of Remote Sensing and Geographical Information System, Guangdong Open Laboratory of Geospatial Information Technology and Application, Guangdong Engineering Technology Research Center of Remote Sensing Big Data Application, Guangzhou Institute of Geography, Guangdong Academy of Science, Guangzhou 510070, China

³ University of Chinese Academy of Sciences, Beijing 100049, China

⁴ Guangzhou Institute of Geography, Guangdong Academy of Science, Guangzhou 510070, China

⁵ Department of Geomatics Engineering, School of Traffic & Transportation Engineering, Changsha University of Science & Technology, Changsha 410114, China

⁶ College of Land Science and Technology, China Agricultural University, Beijing 100083, China

* Correspondence: css@gdas.ac.cn; Tel.: +86-1353-991-9673

Abstract: Lodging is one of the typical abiotic adversities during paddy rice growth. In addition to affecting photosynthesis, it can seriously damage crop growth and development, such as reducing rice quality and hindering automated harvesting. It is, therefore, imperative to accurately and in good time acquire crop-lodging areas for yield prediction, agricultural insurance claims, and disaster-management decisions. However, the accuracy requirements for crop-lodging monitoring remain challenging due to complicated impact factors. Aiming at identifying paddy rice lodging on Shazai Island, Guangdong, China, caused by heavy rainfall and strong wind, a decision-tree model was constructed using multiple-parameter information from Sentinel-1 SAR images and the in situ lodging samples. The model innovatively combined the five backscattering coefficients with five polarization decomposition parameters and quantified the importance of each parameter feature. It was found that the decision-tree method coupled with polarization decomposition can be used to obtain an accurate distribution of paddy rice-lodging areas. The results showed that: (1) Radar parameters can capture the changes in lodged paddy rice. The radar parameters that best distinguish paddy rice lodging are VV, VV+VH, VH/VV, and Span. (2) Span is the parameter with the strongest feature importance, which shows the necessity of adding polarization parameters to the classification model. (3) The dual-polarized Sentinel-1 database classification model can effectively extract the area of lodging paddy rice with an overall accuracy of 84.38%, and a total area precision of 93.18%. These observations can guide the future use of SAR-based information for crop-lodging assessment and post-disaster management.

Keywords: paddy rice lodging; remote sensing; SAR; backscattering coefficient; polarization decomposition; decision tree; disaster



Citation: Dai, X.; Chen, S.; Jia, K.; Jiang, H.; Sun, Y.; Li, D.; Zheng, Q.; Huang, J. A Decision-Tree Approach to Identifying Paddy Rice Lodging with Multiple Pieces of Polarization Information Derived from Sentinel-1. *Remote Sens.* **2023**, *15*, 240. <https://doi.org/10.3390/rs15010240>

Academic Editor: Sang-Eun Park

Received: 3 November 2022

Revised: 26 December 2022

Accepted: 29 December 2022

Published: 31 December 2022



Copyright: © 2022 by the authors. Licensee MDPI, Basel, Switzerland. This article is an open access article distributed under the terms and conditions of the Creative Commons Attribution (CC BY) license (<https://creativecommons.org/licenses/by/4.0/>).

1. Introduction

Global food production must increase by 70% by 2050 to cope with the growth of the world population [1]. Paddy rice is a significant food source in Asia. Its growth process is highly susceptible to adverse meteorological conditions, due to the structural characteristics of the plant. The most common consequence is lodging, which severely impacts rice quality and yield. Studies have shown that when heavy lodging occurs in paddy rice, the yield

reduction rate is probably higher than 20% [2]. Therefore, extensive rice-lodging monitoring is critical for yield forecasts, disaster analysis, and post-disaster remediation.

In general, the conventional methods to assess crop lodging are field-based investigations, which is time-consuming and laborious, and inefficient for large-scale regional surveys and emergency relief [3,4]. Alternatively, remote sensing is recognized as an efficient tool for disaster assessment and has been widely used for crop-lodging detection due to its high scalability and cost-effectiveness [5–7]. Currently, remote-sensing data commonly used for crop-lodging detection include satellite data and unmanned aerial vehicle (UAV) images [8]. UAV images are primarily used to extract lodging information by analyzing the change in texture before and after it occurs. UAVs provide the following advantages: operational flexibility, low economic costs, high spatial resolution, and the ability to acquire cloud-free images [9]. In a previous study, Chauhan et al. [10] assessed lodging impact on paddy rice through UAV imagery with high-resolution multispectral data, where a full convolution neural network technology based on deep learning was used to extract lodging crops from UAV images [11]. A high extraction accuracy has been obtained. However, due to the high cost and technical processing requirements, UAVs are not suitable for regional-scale crop-lodging monitoring. In this regard, satellite-based remote-sensing data, with its ability to have large region coverage, offers a better alternative for lodging monitoring. Broadly, satellite data includes optical satellites, radar satellites, etc. It is widely acknowledged that the difference between lodging and non-lodging areas can be characterized by spectral reflectance and vegetation index—the spectral reflectance increases after lodging, and the vegetation index decreases [12,13]. In this regard, a threshold method was used to extract the lodging paddy rice. In addition, the results of a study by Bao et al. [14] revealed that lodging areas could be distinguished from non-lodging areas based on changes in the spectral reflection characteristics of maize. Using optical data with high spatial resolution, these studies provided good examples of how to track lodging changes within the field. Since paddy rice lodging is often accompanied by cloudy and rainy weather, the optical data lacks spatial/temporal continuity, and the change of canopy spectral information is weak after lodging [15,16]. Therefore, the optical data have certain limitations [17].

Compared to optical sensors, synthetic aperture radar (SAR) has strong penetrability, night acquisition capabilities, and sensitivity to changes in crop structure, which can overcome the deficiencies of optical imaging [18,19]. These qualities provide a clear advantage for continuous lodging monitoring. Remote-sensing research on rice lodging can be divided into two directions: (i) distinguishing lodgings and non-lodgings [18]; (ii) classification of lodging severity [16]. However, there are still large challenges in increasing the accuracy of crop-lodging detection from remote-sensing data. At present, most studies on crop-lodging monitoring mainly focus on wheat and maize, rather than paddy rice [3]. Another problem is that most studies mainly focus on using more expensive quad-polarization SAR data, overly relying on the backscattering coefficient [20], and the polarization parameters involved in polarization decomposition are underused.

Acknowledging these gaps, this study explored the potential capability of dual-polarized SAR data with backscattering coefficients and polarization decomposition parameters to assess the paddy rice-lodging area. A decision-tree method has been developed and compared with other methods. The present study analyzed the sensitivity of each parameter to lodged paddy rice and then quantitatively assessed the importance of the optimal parameters based on RF and XGBoost. In addition, the model's mechanisms and uncertainty were assessed.

2. Materials and Methods

2.1. Study Area and In Situ Measurements

The study area, Shazai Island, is in the center of the Tam River (Figure 1a), Xinhui District, Guangdong Province, China (22.39°–22.43°N, 113.06°–113.07°E), with a total land area of 245.5 hectares (including 167.3 hectares within the embankment). It is an alluvial

island suitable for cultivating farmland, featuring a sub-tropical marine climate. Field parcels are homogeneous and flat, and the plant structure is simple. Paddy rice usually grows in patches, and is harvested twice a year. A demonstration base for organic paddy rice production has been established in Shazaichang, Sanjiang Town. In the study site, early rice is generally sown around 15 March, and harvested around 15 July. Due to mechanized cultivating, soil fertility in the area is homogeneous.

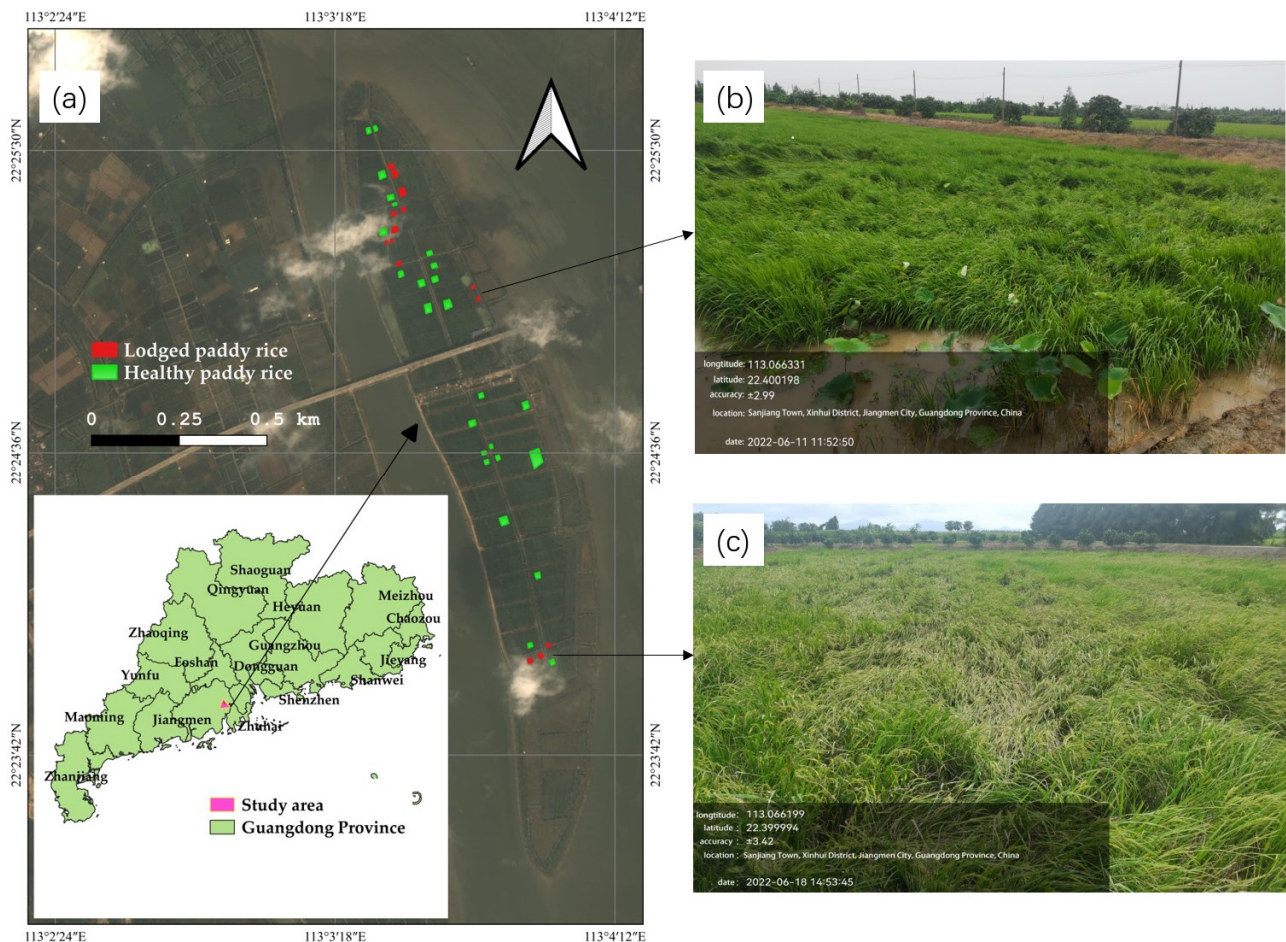


Figure 1. Study area description. (a) the location of the study area in Xinhui District, Guangdong Province, China, and the sampling site (Red is the lodging area. Green is a no-lodging area); (b,c) two typical lodged paddy rice fields investigated on 11 June, and 18 June 2022.

In June 2022, South China encountered a typical meteorological disaster that was nicknamed “Dragon Boat Rain”, a reference to heavy precipitation around the Dragon Boat Festival that occurs around the summer solstice (between 21 May and 20 June). Crops in many regions suffered varying degrees of damage due to heavy rainfall for a prolonged period of time. Additionally, the island is open on all sides, which led to severe paddy rice lodging (Figure 1b,c). From field surveys carried out on 11 June 2022 and 18 June 2022, 46 ground data were collected (Figure 1a). A handheld GPS was used to collect the longitude and latitude of the samples and the data were saved as shapefile format.

Paddy rice lodging occurred twice in the study area during the Dragon Boat Rain of 2022. According to meteorological station records, the first lodging occurred due to heavy rain (58.1 mm/d) that took place on 8 June 2022, and a high-speed wind (4.8 m/s) on 18 June 2022 (as shown in Figure 2). It is consistent with the field survey results. Based on paddy rice phenological staging on Shazai Island [21] (Figure 3), there is a milking stage when rice lodging.

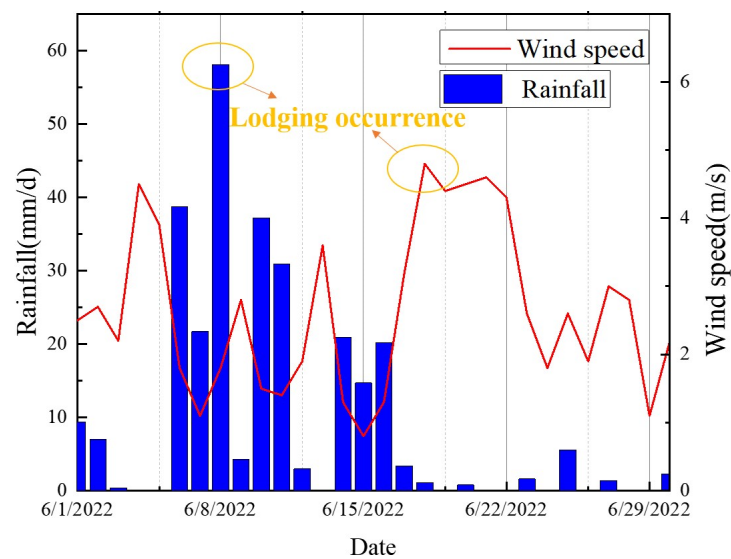


Figure 2. Corresponding daily cumulated rainfall (mm/d) and daily average wind speed (m/s) on Shazai Island during the “Dragon Boat Rain” of 1 June to 30 June 2022.

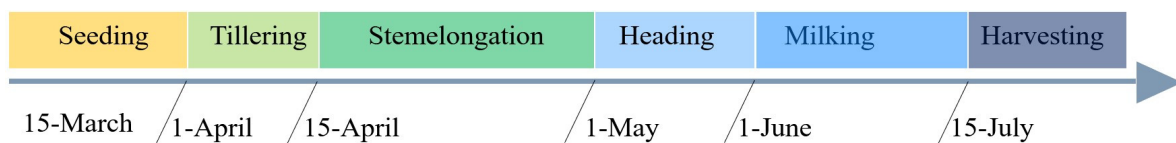


Figure 3. Early paddy rice phenology in Shazai Island.

2.2. Data and Preprocessing

2.2.1. Remote-Sensing Data and Preprocessing

The radar data used for the study were downloaded from the C-band SAR sensor on board the Sentinel-1A satellite from the European Space Agency’s Copernicus program GMES (Global Monitoring for Environment and Security) (<https://scihub.copernicus.eu/> (accessed on 20 December 2022)). Both Ground-Range Detected (GRD) and Single-Look Complex (SLC) images were used in Interferometric Wide-Sweep mode (IW). GRD and SLC contain modes of dual polarizations (VV, VH), where H represents horizontal polarization and V represents vertical polarization. As Level-1 products, these images have a spatial resolution of 22 m in azimuth and 20 m in range direction, as well as a pixel spacing of 10×10 meters. The GRD products were processed to obtain Sigma naught. Complex data were used to retain phase information in SLC products, and sufficient signal bandwidth helps achieve single-view processing.

Preprocessing of the GRD data was performed using the Sentinel-1 Toolbox in SNAP 9.0, which included applying orbit file, removing GRD border and thermal noises, radiometric calibration, and orthorectification [22]. The preprocessing of SLC images was conducted in polSARpro 6.0.3 [23]. First, we extracted the real and imaginary images in the complex data and synthesized them into amplitude images, after which the covariance matrixes (C2) were generated. To suppress the inherent speckle noise of images, the multi-look method with a factor of 4 in range and 1 in azimuth directions was used to generate a square pixel. Furthermore, the spatial filter was conducted by a 7×7 Refine Lee filter. Finally, all polarization matrixes were geocoded into the Universal Transverse Mercator (UTM) map projection using external SRTM DEM data (30 m spatial resolution). Based on geocoded data, five polarimetric parameters were calculated (Alpha, Anisotropy, Entropy, Shannon, and Span).

Therefore, a synchronous date for the ground-truth data acquisition was selected for the GRD and SLC products of Sentinel-1 data. Their specific parameters are listed in Table 1.

Table 1. Sentinel-1 data used in this study.

Satellite	Data	Resolution	Work Pattern	Flight Direction	Incidence Angle
Sentinel-1A (GRD)	2 June 2022 (pre-lodging image)	10 m	Interferometric Wide swath (IW)	Ascending	39.15°
	24 June 2022 (post-lodging image)				
Sentinel-1A (SLC)	2 June 2022 (pre-lodging image)	10 m	Interferometric Wide swath (IW)	Ascending	39.15°
	24 June 2022 (post-lodging image)				

2.2.2. Other Data

Gaofen-6 images of high resolution are freely available, which meet the requirements of acquiring farmland plot boundaries. The high-resolution images (2 m spatial resolution) were downloaded from China Center for Resources Satellite Data (CCRS) (<http://218.247.138.119:7777/DSSPlatform/index.html> (accessed on 20 December 2022)). In addition, the Gaofen-6 images were combined with recently available Sentinel-2 multispectral data from GMES to produce a base map of paddy rice plant areas. Additional statistics on the rice paddy plant area and damaged paddy rice on the island were collected by visiting local farmers (Table 2).

Table 2. Summary statistics of the disaster from measurement data from local farmers.

Years	Paddy Rice Plant Area (ha)	Paddy Rice-Affected Area (ha)	Lodging Ratio
2022	123	22	17.89%

Lodging ratio is the percentage of lodging paddy rice to healthy paddy rice.

2.3. Methods

SAR backscattering coefficients and polarimetric parameters are influenced by many factors, including leaf density, structure, water content, variety, and phenological periods [24]. The following polarization information can enhance lodged paddy rice identification susceptibility: the ability to reduce the environment's effects, crop growth variation, and system bias [25]. Lodged and healthy paddy rice presents different scattering mechanisms mainly due to differences in structure and water content. Therefore, the SAR data were processed so that their electromagnetic wave intensity and phase information could reflect the characteristics of the backward-scattering coefficients and polarimetric parameters.

Since the study area is small and paddy rice grows in patches, this paper outlines the paddy rice-growing area using a high-resolution Gaofen-6 image and synchronous Sentinel-2 multispectral data to eliminate the bias caused by other plots and environmental factors. We selected the in situ data of 14 lodging samples (L1–L14) and 25 healthy samples (H1–H25) (Figure 1). The average of the backscatter coefficients and polarimetric parameters were calculated at the parcel level to overcome heterogeneous noise in SAR data. We used the preprocessed GRD and SLC products to obtain SAR polarization information.

2.3.1. Selection of Optimal Feature Parameters

A. Construction of feature parameters

The five backscatter coefficients (VV, VH, VV+VH, VV-VH and VH/VV) have been proven sensitive to crop lodging [26]. To fully use the polarization information, we extracted polarization decomposition parameters. For Sentinel-1 dual-polarized data, the current polarization decomposition technology is $H/\alpha/A$ decomposition, as proposed by Cloude [27]. Polarimetric decomposition parameters were used to separate the crop contributions from the total backscatter. The differentiating potential of these three parameters (Alpha, Anisotropy, and Entropy) for lodging crops has been confirmed in Shu and Wang's study [14,17]. Additionally, it is important to note that Shannon and Span are sensitive to crop structure. At present, little research on lodging has been conducted on the

10 parameters, especially in southern China. We conduct a comprehensive analysis of the above 10 parameters. The 10 parameters are extracted as follows.

The backscattering coefficients VV and VH (in dB) were obtained by preprocessing the GRD product, after which a linear combination based on ArcGIS was conducted to calculate feature parameters: VV+VH, VV-VH, and VH/VV.

For the polarization decomposition of the dual-polarized data, we used H/ α /A polarization decomposition to extract Alpha, Anisotropy, and Entropy parameters for all the sample plots, using the confusion matrix and eigenvalue decomposition. Eigenvalue decomposition has the significant advantage of not being limited by the specific scattering mechanism, and the eigenvalues do not change when the antenna coordinate system is transformed. Therefore, it is the most effective for the decomposition of naturally distributed target scattering. Specifically, we also extracted the polarization feature Shannon, and Span. Ten feature parameters (VV, VH, VV+VH, VV-VH, VH/VV, Alpha, Anisotropy, Entropy, Shannon, and Span) were generated from Sentinel-1 A images. The presentation of each parameter is shown in Table 3.

Table 3. SAR backscattering coefficients and polarimetric parameters.

Features	Formula	Meaning
Backscattering coefficients [18]	VV, VH, VV+VH, VV-VH, VV/VH	Backscattering coefficients and their linear combinations.
Alpha [19]	$Alpha = \frac{1}{\lambda_1 + \lambda_2} \sum_{i=1}^2 \lambda_i \alpha_i$	The type of scattering mechanism (when $\alpha \rightarrow 0$ corresponds to single scattering from rough surfaces; $\alpha \rightarrow \pi/4$ indicates volume scattering; $\alpha \rightarrow \pi/2$ corresponds to double-bounce scattering).
Entropy [19]	$-\sum_{i=1}^2 P_i \log_2(P_i)$	The proportion of each scattering mechanism in the overall scattering process (ranging from 0 to 1). It also represents the randomness of the scattering process from isotropic scattering ($H = 0$) to random scattering ($H = 1$).
Anisotropy [19]	$\frac{\lambda_1 - \lambda_2}{\lambda_1 + \lambda_2}$	A complementary parameter to Entropy represents the difference between the second and third eigenvalue mechanisms. It can be used to assess the structural and spatial homogeneity of a target.
Shannon [14]	$2 \log(\frac{\pi e Tr[C_2]}{2}) + \log(4 \frac{\det[C_2]}{Tr[C_2]^2})$	The sum of scattering intensity, which can reflect the rich information contained in polarized interferometric SAR.
Span [14]	$ C_{11} ^2 + 2 C_{12} ^2 + C_{22} ^2$	The total scattered power.

B. Lodging factors and consistency analysis.

We constructed the lodging factor criterion γ and the consistency detection criterion (β and ε) for changes in lodged paddy rice parameters to select the most sensitive parameters for lodged paddy rice [14]. The following steps were taken for selecting the optimal parameters.

First, the paddy rice-lodging factor criterion γ was constructed to find parameters that have significant changes before and after lodging.

$$\gamma = \left| \frac{LB_{av} - LA_{av}}{LB_{av} + LA_{av}} \right| - 1.5 \left| \frac{HB_{av} - HA_{av}}{HB_{av} + HA_{av}} \right| \quad (1)$$

where LB_{av} ($LB_{av} = (L1 + L2 + \dots + L14)/14$) is the mean value of 14 lodged paddy rice samples before the lodging. LA_{av} ($LA_{av} = (L1 + L2 + \dots + L14)/14$) is the mean value of 14 lodged paddy rice samples after the lodging; HB_{av} ($HB_{av} = (H1 + H2 + \dots + H25)/25$) is the mean value of 25 healthy paddy rice samples before the lodging. HA_{av} ($HA_{av} = (H1 + H2 + \dots + H25)/25$) is the mean value of 25 healthy paddy rice samples after the lodging. When γ is greater than 0, the parameters changed more before and after lodging than healthy paddy rice did. Therefore, we defined parameters with γ greater than 0 as those with sufficient sensitivity to lodged paddy rice.

Second, two parameters (β and ε) were constructed to analyze the trends of SAR backscatter coefficients and polarimetric parameters of all lodged paddy rice plots, as follows:

$$\varepsilon_i = LA_i - LB_i (i = 1, 2, \dots, 14) \quad (2)$$

$$\beta = \text{sign}(\varepsilon_i) \quad (3)$$

where ε_i is the difference between the parameter values LA_i (samples after the lodging) and LB_i (samples before the lodging); β is the sign number of ε_i with higher frequency, and the larger its value, the higher the consistency of change across samples for this parameter after the lodging. We denoted $\beta \geq 12$ as good consistency of the selected parameters for the change in the lodged paddy rice.

2.3.2. Construction of Decision Tree

Based on the discriminant analysis, the optimal sensitivity parameters were selected to build a decision-tree classification model for extracting the distribution of lodged paddy rice. To obtain more-accurate classification results, it is necessary to further explore whether the selected parameters can differentiate between lodged and healthy paddy rice. We constructed a boxplot to perform the discriminant analysis, which can visually represent the degree of dispersion and distribution of data and can highlight abnormal data. The optimal features to discriminate different categories can be selected by comparing the boxplot of the same feature between lodged and healthy paddy rice. The classification thresholds between lodged and healthy paddy rice were obtained by visual inspection. Finally, the threshold-based methods employed a hierarchical decision tree to combine the unique characteristics of paddy rice scattering. The techniques have substantial advantages, such as intuitive simplicity, flexibility and good computation efficiency. The methodological flowchart is shown in Figure 4.

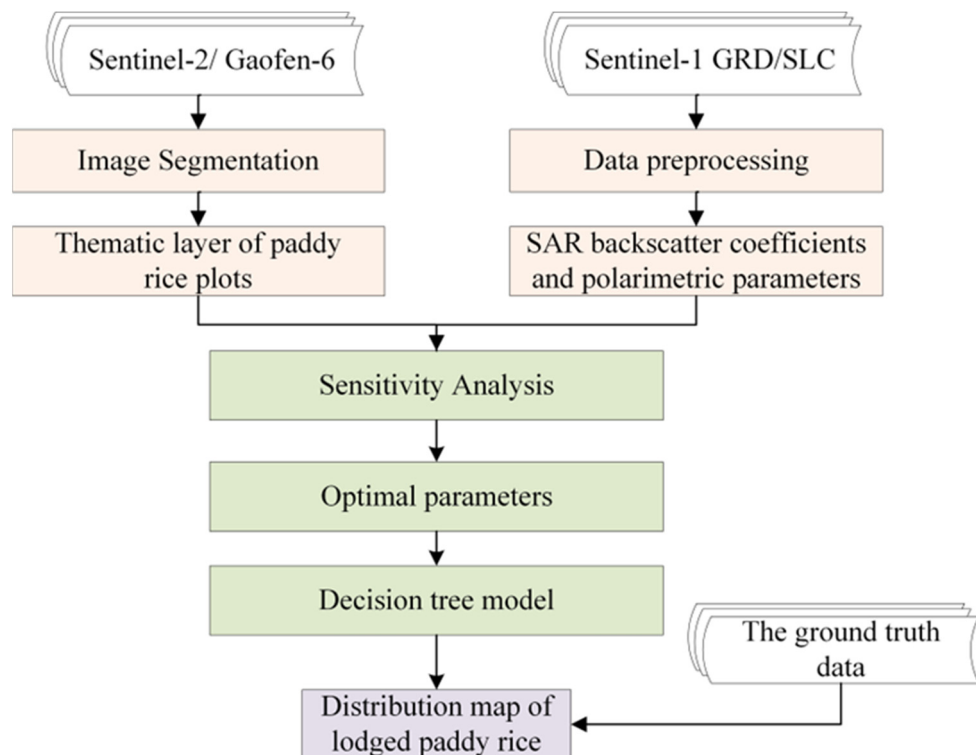


Figure 4. Methodological flowchart for extracting the distribution map of lodged paddy rice using remote-sensing imagery.

2.3.3. Accuracy Evaluation Method

For accuracy analysis of the classification results, we used field sampling data and disaster statistics as quasi-true values to construct two evaluation methods: error matrix evaluation and area accuracy evaluation. The two methods were used to evaluate the classification results from the two aspects of field positioning and regional statistics quantification, respectively. User accuracy (UA), producer accuracy (PA), overall accuracy (OA), and kappa coefficient of classification results were calculated using a confusion matrix [28], which reflected the positional accuracy of classification results in the study area. On the other hand, based on a comparison of the lodged paddy rice area with disaster statistics data, the total area precision (P_s) was determined by applying Formula (4) [29]:

$$P_s = 1 - \frac{|A_i - A_0|}{n} \times 100\%. \quad (4)$$

where A_i is the area of lodged paddy rice in the study area, and A_0 is the quasi-true value (statistics value) of the area of paddy rice damage counted by the field observations.

2.3.4. Sensitivity Analysis of Optimal Features

Feature importance (FI) analysis is an effective approach used in model interpretation [30], which estimates the contribution of each feature to the model's classification result. Random Forest and eXtreme Gradient Boosting (XGBoos) algorithms were used to measure the "importance" of features [31], developed in the Python programming environment.

Random Forest is a bagging-based ensemble classifier consisting of multiple fully grown decision trees. According to gain maximization, the features with the best classification ability are obtained. The present study evaluated FI based on the classification accuracy of out-of-bag data (OOB). The process of analysis is as follows: (1) Constructing M decision trees, with $k_{\text{tree}} = 1$ initially and using auto-resampling to generate the training set and out-of-bag data set (OOB_k); (2) Calculating the $errOOB_k$ of the current decision tree for OOB_k ; (3) Calculating the $errOOB_k^i$ of the i -th feature; (4) Repeating the above steps for each decision tree; and finally (5) The FI of each feature is calculated according to Formula (5). If the classification accuracy does not change much before and after the perturbation, it indicates that the feature plays a small role in classification and the classification performance is low.

The higher the score, the larger the influence that the specific feature will have on the model used to predict a certain variable.

$$Score_{RF} = \frac{1}{M} \sum_{k=1}^M (errOOB_k^i - errOOB_k) \quad (5)$$

where M is the number of decision trees, and $errOOB_k^i$ and $errOOB_k$ represent the prediction errors of the OOB data after adding perturbation to the i -th feature and the OOB data without perturbation in the case of the k_{tree} decision tree.

In the machine-learning algorithm XGBoost, part features were selected to construct a simple decision-tree model. A new model was generated by learning the residuals of the simple model and minimizing the objective function. By repeating this process, many simple models were produced and combined into a comprehensive model with higher accuracy. The algorithm calculated the importance of features mainly through three standards: gain, frequency, and coverage. Frequency is a simplification of gain, measured by the number of times a feature occurs in all constructed trees. Coverage is the relative value of a feature. Gain is the main reference factor to determine the importance of branch features, and it is the most relevant factor for explaining the importance of each feature. Therefore, we calculated the importance of features by gain in this study. The best split point represents the maximum gain. Good features can improve the mean square difference on a single tree. The more improvements, the better the splitting point, the more important this feature is. For instance, for a single tree T , if the j -th feature is selected as

the split variable on this tree, the sum of mean square difference on all branch nodes t is calculated. The importance of the j -th feature on the tree is as follows:

$$I_j^2(T) = \sum_{t=1}^{j-1} i_t^2 P(v_t = j) \quad (6)$$

where i_t^2 is the improvement of squared difference of the node t , and v_t is the feature associated with node t . By summing and averaging the importance of the j -th feature on each tree, the final feature importance score with M trees can be obtained from Formula (7):

$$Score_{XGBoost} = \frac{1}{M} \sum_{m=1}^M I_j^2(T_m) \quad (7)$$

3. Results

3.1. Feature Separability for Lodged and Healthy Paddy Rice

The difference between each parameter before and after the disaster was calculated for each sample to determine which parameters best separated lodged paddy rice from healthy paddy rice, and the sample mean and 95% confidence interval were calculated. The results are shown in Figure 5. Alpha is the only one with a confidence interval of zero in all the parameters. This indicates that most of the parameters have dispersion ability for lodged and healthy paddy rice. The results showed that the values of VV, VH, VV+VH, VV-VH, VH/VV, Shannon, Anisotropy and Span increased after the lodging. The VV and VH value increased by 3.79 dB and 2.14 dB, respectively, and similar backscatter coefficient behavior can be observed in other cereals such as wheats [32]. The Shannon and Span value increased by 1.08 and 0.01, respectively. In contrast, the values of Entropy decreased 0.06 after the lodging. The increase in VV has been attributed to the fact that the vertical structure of the paddy rice stalk was disrupted by the lodging, resulting in the reduction in the attenuation of V poles by the stalk. The increase in VH was due to increased volume scattering and vegetation–soil bidirectional reflection scattering, caused by changes in crop canopy structure [32,33]. There was a significant increase in VV compared to VH. This is possibly because the changes of the vertical structure of paddy rice stalk after lodging have more impact on SAR polarization parameters than the changes of canopy structure. Finally, the VV backscatter coefficient is the main component of the total backscatter signal [34].

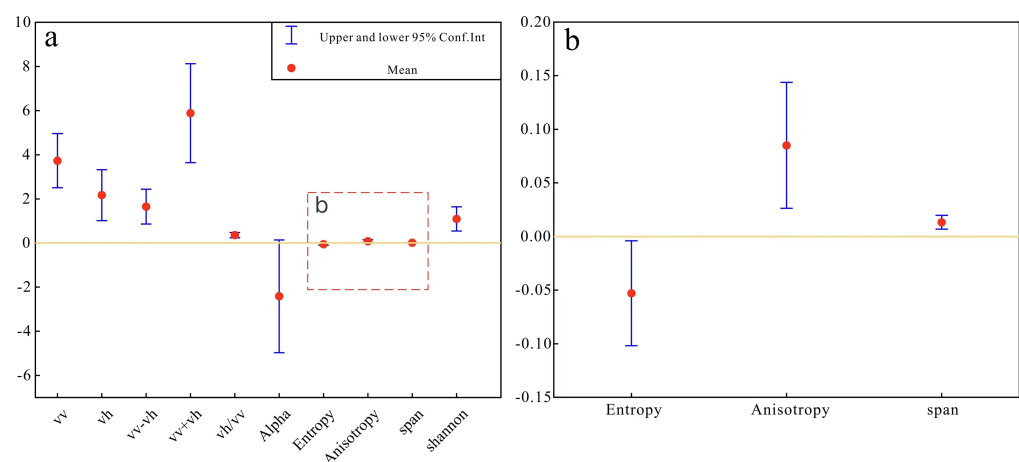


Figure 5. The interval graph represents the range of the radar characteristic parameters of the paddy rice samples before and after the disaster. As the values of Entropy, Anisotropy and Span are small, the intervals are not obvious under the scale (a). Therefore, with the change of axis range, the stretching result will change (b). The yellow line represents the threshold of 0. If the interval includes a 0 value, it means that the separability is not significant.

3.2. Analysis of Lodging Factors and Their Consistency

The lodging factors and consistency were plotted in a scatter plot (Figure 6). It can be found that Span, Shannon, VH/VV, VV, VV-VH, VV+VH, VH, Anisotropy, Alpha, and Entropy meet the condition $\gamma > 0$, and the γ values decrease in order. A larger γ value indicates that the difference between lodged and healthy paddy rice for this parameter is greater and more sensitive to lodged paddy rice extraction. The γ values for VH, Anisotropy, Alpha, and Entropy are low, meaning that the four parameters do not change significantly after the paddy rice lodging. The numbers of the sign of ΔVV , $\Delta(VV+VH)$, $\Delta(VH/VV)$, and Δ Span (the difference of polarization parameters before and after the lodged samples) meet $\beta \geq 12$, indicating that the parameter changes are consistent. Despite the high Anisotropy, it does not have a high consistency; therefore the Anisotropy is excluded from the study. Finally, the optimal parameters that meet the conditions were obtained: VV, VV+VH, VH/VV, and Span. In this study, Alpha, Anisotropy, and Entropy are not sensitive to lodged paddy rice, probably due to the lack of partial polarization information in the dual-polarized data [14]. The scatter plot indicates that the higher the values of lodging factor and consistency, the closer they are to the upper right corner of the plot, which was best for modeling requirements.

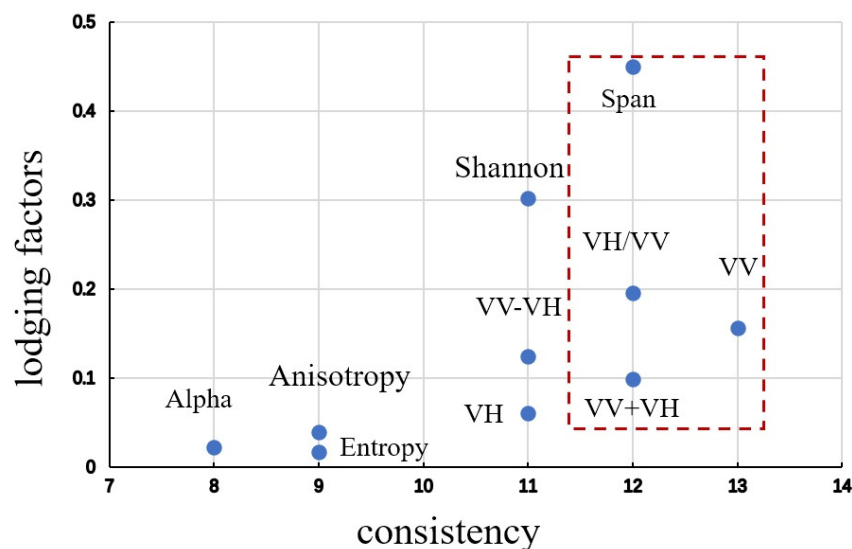


Figure 6. Scatter graph representing the lodging factor (γ) and consistency detection criterion (β) of the ten SAR characteristic parameters. The optimal four parameters that meet the conditions are highlighted with red boxes.

3.3. Production of Decision Tree

The optimal sensitivity parameters of lodged paddy rice were obtained using sensitivity criterion analysis (γ) and consistency detection criterion (β). On the box plots (Figure 7), VV has the highest separation ability since its value has the largest difference. The minimum value of VV of lodged paddy rice is greater than 3/4 of the value of healthy paddy rice, and the average value of lodged paddy rice is almost greater than the maximum value of healthy paddy rice. All parameters of lodged paddy rice were higher than those of healthy paddy rice. The reason for this is that the changes in vegetation due to lodging become evident under the change in its biophysical/biochemical properties (e.g., reduction in crop height, moisture change in vegetation, etc.).

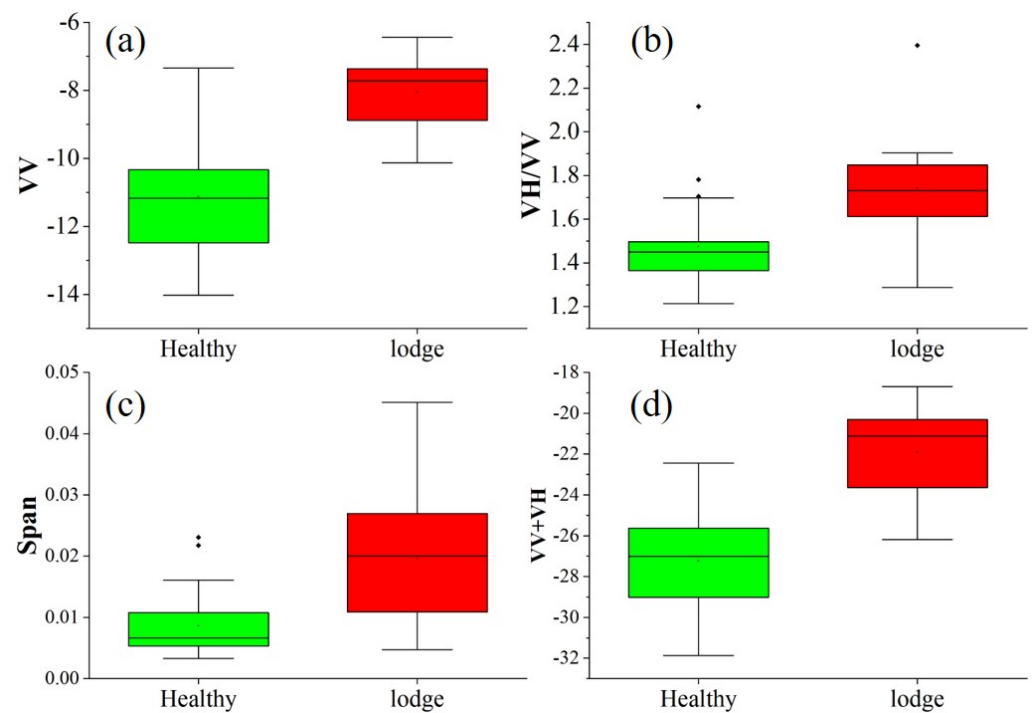


Figure 7. The variation of VV (a), VV+VH (b), VH/VV (c), and Span (d) for healthy and lodged paddy rice.

Based on the above boxplot, the VV with the best separation was selected as the first level of the decision tree, followed by VV+VH, Span, and VH/VV, sequentially. To ensure that the threshold can cover all lodged paddy rice, lodged paddy rice is defined as having a VV greater than -10 , while healthy paddy rice is defined as having a VV less than -10 . The iteration was then carried out using the following rules: $VV+VH > -26$, $\text{Span} > 0.01$ and $VH/VV > 1.5$. Finally, the decision tree (Figure 8) was constructed in ENVI for the classification of healthy and lodged paddy rice plots.

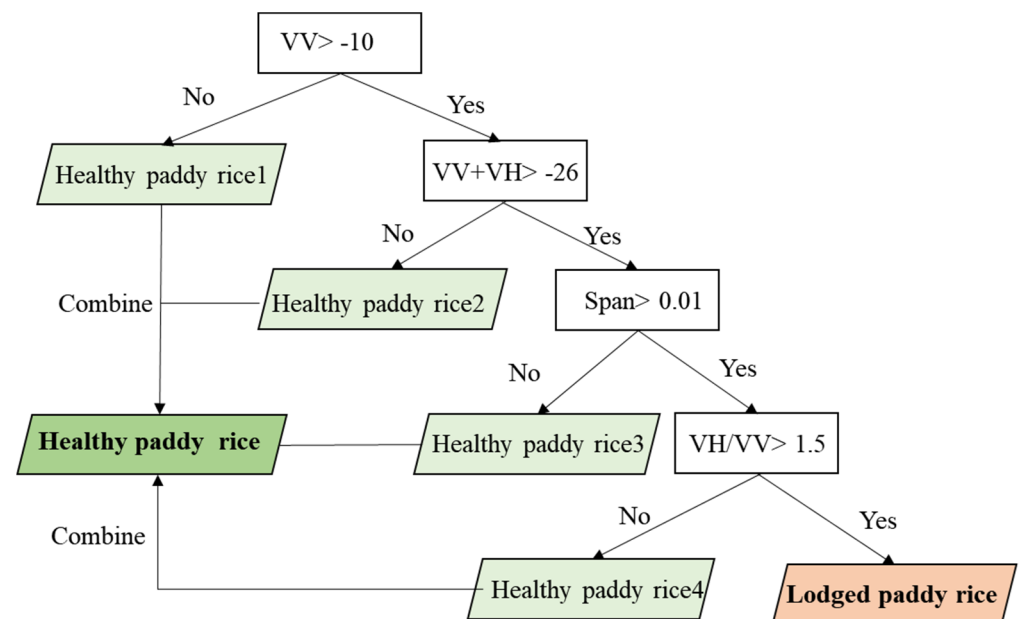


Figure 8. Decision-tree model for classification of healthy and lodged paddy rice.

3.4. Spatial Distribution of Lodged Paddy Rice

The area of early rice planted on Shazai Island was about 113 hectares in 2022, and the area planted on the south and north islands was approximately equal. The decision-tree classification was carried out using the sensitivity parameters of lodged paddy rice including backscattering coherences and polarimetric parameters, and the classification results are shown in Figure 9, where the lodged paddy rice area was about 20.5 ha, and the lodging rate was about 18.14%. The in situ surveyed lodging rate was 17.89%, and the overall lodging results were basically consistent with the field survey results. It can be seen from Figure 9 that there is an uneven distribution of lodged paddy rice. From a south–north perspective, the severe lodged areas were concentrated in two plots in the northern part of the study area, whereas they were scattered in the southern part. From an east–west perspective, most lodging occurred on the eastern side of the island, particularly at the edges of plots. In the west of islands, the lodged paddy rice is rare.



Figure 9. Map of lodged paddy rice extraction results.

3.5. Accuracy Analysis

A confusion matrix was built to evaluate the accuracy of the two classification results (Figure 10). This method can classify lodged and healthy paddy rice with an overall classification accuracy (OA) of 84.38% and a kappa coefficient of 0.62. Producer accuracy

(PA) for healthy paddy rice is 85.71%, while lodged paddy rice is 80.65%. The user accuracy (UA) is 67% for healthy paddy rice and 92.5% for lodged paddy rice. In the north–south direction, the classification accuracy in the north was significantly higher than the south. The overall classification accuracy in the north was 90.87%, while the classification accuracy in the southern region was 75.18%. The high classification accuracy in the north is probably due to the differences in growth periods and lodged samples.

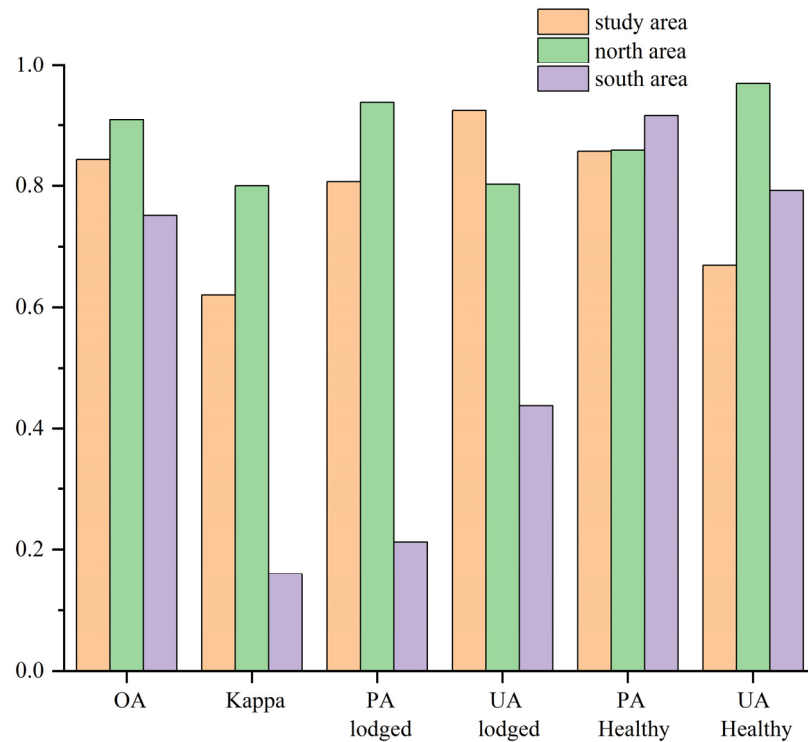


Figure 10. Accuracy evaluation results for different regions (the entire study area, north part, south part).

According to the area accuracy evaluation, the total area precision (P_s) of lodged paddy rice was 93.18%. It indicates that the extracted total area of lodged paddy rice is highly consistent with the actual area of lodged paddy rice.

We also compared the proposed method with four other methods, including the IsoData and K-Means classification of the supervised classification algorithm, and the Minimum Distance classification, and Support Vector Machines of the unsupervised classification algorithm. The results (Table 4) showed that our method can generally better balance omission and commission errors, as the produced results show a higher UA and comparable PA compared with other methods [28]. Compared to supervised classification methods, the method achieves high classification accuracy and does not require a lot of sample data, therefore reducing the cost.

Table 4. Accuracy assessment of four methods: user's accuracy (UA), producer's accuracy (PA), overall accuracy (OA) and kappa for the paddy rice-lodged class.

Classification Methods	Healthy Paddy Rice		Lodged Paddy Rice		OA (%)	Kappa
	UA (%)	PA (%)	UA (%)	PA (%)		
IsoData	72.22%	52.00%	42.86%	65.28%	0.56	0.20
K-Means	88.23%	62.50%	57.14%	85.71%	0.71	0.47
Minimum Distance	85.71%	72.00%	61.11%	78.57%	0.74	0.45
SVM	84.00%	84.00%	71.42%	71.43%	0.79	0.43
Decision Tree	87.50%	84.00%	73.30%	78.57%	0.85	0.65

3.6. Sensitivity of Optimal Features

Through the scikit-learn package in Python, the feature importance scores were obtained based on Random Forest and XGBoost. The results are shown in Figure 11, which indicates that the results of the two algorithms are consistent. Obviously, Span has the highest score, representing that it is the most important feature with better classification performance, followed by VH/VV, VV, VV+VH sequentially. The other three features are equally important. It is likely that the Span has excellent classification performance because it follows the intrinsic characteristics of lodging rice and has good anti-inference abilities, including the ability to resist the influence of vegetation water content and growth differences [23].

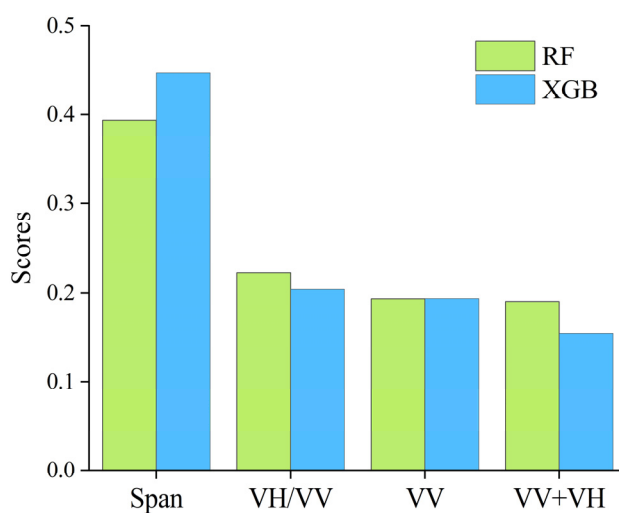


Figure 11. Statistical results of feature importance scores (Span, VH/VV, VV, VV+VH).

4. Discussion

4.1. The Radar Mechanism of the Decision Tree Based on Feature Parameters

Microwave scattering is mainly determined by crop macrostructure (planting density, underlying soil moisture) and canopy structure (the dielectric properties of crop canopy, crop moisture content as well as leaf size) [35,36]. Three types of scattering mechanisms can occur when a microwave signal hits a crop canopy: surface/single-bounce, double-bounce, and volume scattering. The decision tree based on polarization parameters proposed in this paper takes full advantage of the sensitivity of SAR polarization features to structural changes in lodged paddy rice. Backscattering coefficients and polarization parameters changed due to the asymmetric polarimetric behavior of lodged paddy rice, compared with the symmetric behavior of standing paddy rice in the azimuth direction [36]. Specifically, the sensitivity of VH is lower than VV, and VV+VH in paddy rice-lodging monitoring [14,15], while VH is more sensitive to wheat lodging [33]. This may be due to surface scattering being typically strongest in VV mode [36]. In addition, the combination of scattering information and polarization parameters can improve the detection capabilities of lodged crops [20]. With the polarization parameters proposed in our study, the effect of crop growth stages can be eliminated by reducing the impact of absolute total power [11]. Anisotropy is not sensitive to lodged paddy rice since it reveals the strength of secondary scatter only when $0.7 < \text{Entropy} < 0.9$. Anisotropy has little effect in this situation due to the low Entropy. However, the polarization parameter (Span) shows excellent classification ability. Many factors may contribute to this, including the fact that it contains the full power of radar echo reflecting the intrinsic characteristics of lodging crops, and has superior anti-inference ability, such as resisting the influence of vegetation water content, growth difference, etc.

It should also be noted that the effect of water content can be ignored since the SDWI (Sentinel-1 Dual-Polarized Water Index) decreased after the paddy rice lodging (see Figure A1). Furthermore, soil surface scattering is dominant during early season when crop

cover is low. With the increase of vegetation coverage density, microwave scattering cannot penetrate the plants and detect the moisture content of the underlying surfaces [36].

4.2. Performance of the Decision-Tree Models for Paddy Rice-Lodging Classification

The reasonable performance of the classification of lodged paddy rice distributions using the decision-tree models is demonstrated by the confusion matrix and measured or statistical data. The optimal sensitive parameters VV, VH, VH/VV, and Span were selected for separating healthy and lodged paddy rice. Nevertheless, there are still some misclassifications. The misclassifications and the reasons for lodging were analyzed. Paddy rice lodging in the study area was heterogeneous. The areas with severe lodging were concentrated in two fields in the north of the study area. This was because the paddy rice in the north was sown earlier, and the field contained many seeds left by last year's late rice, which was already in the milk-ripening stage, with a higher growth vigor, and was more prone to lodging in strong wind and heavy rain [37]. A further finding was that paddy rice was grown more densely in the north than in the south. As a result of dense plant tillering and competition for limited resources (nutrients, sunlight, etc.), lodging was more likely to occur [38,39]. From an east–west perspective, the lodging areas are mainly located on the eastern side of the island, due to being close to Yamen waterway with east-to-west winds. On the other hand, the low-lying terrain in the southern part of the study area caused the accumulation of water, which delayed the phenological development of paddy rice. Southern paddy rice was misclassified in the stage of stem elongation due to differences in crop growth. Therefore, the built decision-tree model may be more appropriate for the lodging assessment during the stages of heading and milking. Furthermore, field surveys have shown that there were some unreasonable lodgings at field edges because of mixed-image pixels caused by unclear plots and road boundaries. Overall, the performance of the decision-tree classification model is affected by these factors (growth stage, plant density, windspeed, etc.).

In recent years, with the rise of big data and artificial intelligence, more and more scholars have turned to machine-learning methods to build remote-sensing analysis models [15,40]. In addition, it is generally accepted that machine-learning models have higher accuracy and better performance. Traditional empirical models such as linear regression and decision trees have weak predictive power compared to machine-learning methods and cannot model the inherent complexity of the dataset. However, empirical models are easier to understand and explain, which is an inherent property of the model. Consequently, there is a trade-off between accuracy and interpretability here. An extraction accuracy of 84.38% was obtained using a relatively simple decision-tree model here. Compared with Wang's random forest method, which has an accuracy of 88% for identifying lodged paddy rice [14], the study shows that the traditional empirical model and machine-learning model can maintain high consistency in extracting lodged paddy rice [41].

4.3. Advantages and Applications of the Method

Remote-sensing communities should build stronger links with end users, which is important for successful integration of Earth observation products into crop-lodging assessment. The application of remote-sensing methods to monitor paddy rice-lodging disaster is a part of agronomic intelligence. The proposed method, for example, can be used to quickly extract lodged crops for agricultural insurance claims using a small number of field samples, which greatly saves time and labor costs. Meanwhile, an accurate lodging location gives farmers useful information for arranging rescue measures and reducing yield losses. In addition, it can be applied to other upright cereal crops such as wheat, corn and sugarcane, given similar radar scattering behavior [3,41,42]. The proposed method is of probably universality for different crops to identify sensitive parameters, although their varied morphological structure and growth environment result in differences in sensitive parameters. Above all, compared with other methods, the proposed method

has the advantage of requiring few samples and providing comparable accuracy and interpretability.

4.4. Uncertainties

There are still several issues with SAR data application in crop-lodging classification. First, this paper's classification results are dependent on first-stage sample size and representativeness. Therefore, it is necessary to develop a classification model that is more universally applicable. The algorithm also needs to be tested in a wider area with complex planting structures. Second, the field survey found that the most severe form of lodging is a crop close to the milking stage [3]. The paddy rice lodging study in this paper is limited to the milking stage and part of the heading stage. It lacks data validation in multiple areas, and the stability of the model needs to be tested. Alternatively, the unprecedented availability of dense time-series of SAR data with high spatial resolution presents a new opportunity for operational assessment of crop lodging in almost real-time. During a crop's growing season, polarization information can be captured dynamically to reveal crop morphology, structure, growth and disaster conditions [43]. Therefore, a combination of long-term time-series SAR data and paddy rice phenological information could be used in future studies. In addition, the method does not consider meteorological conditions, as well as other management-related factors. Several factors should be considered when analyzing the impact on yield. Moreover, the Sentinel-1A satellite data contains only two polarization modes. It is necessary to further study the quad-polarized radar with more scattering information for monitoring paddy rice lodging. Additionally, an effective combination of optical images for quantitative lodging calculations will be an important research direction for SAR applications in crop lodging. Furthermore, research on the impact of environmental factors, such as soil moisture and windspeed on the classification method, should be considered, which are lacking in this study.

5. Conclusions

In this study, we designed a new decision-tree method based on the backscattering coefficients and polarimetric parameters of dual-polarized Sentinel-1 data to distinguish lodged paddy rice from healthy paddy rice. The key conclusions are summarized below:

(a) The proposed method can achieve an accurate classification map of lodging paddy rice with an overall accuracy of over 84.38%, and an area-classification accuracy of 93.18%, which is comparable to other methods.

(b) The backscattering coefficients VV, VH, VV+VH, VV-VH, and VH/VV increase in general after paddy rice lodging, and the polarization parameters Shannon and Anisotropy, Span also increases to varying degrees. On the contrary, the polarization parameters Alpha and Entropy decreased after paddy rice lodging.

(c) The backscatter coefficients VV, VV+VH, VH/VV, and the polarimetric parameter Span of the dual-polarized SAR data are more sensitive to lodged paddy rice. The feature importance assessment shows that Span has the highest sensitivity, which means it is the most important parameter for the classification model.

Above all, the five backscattering coefficients and five polarimetric parameters when incorporated into a decision-tree model can provide referred application for accurate paddy rice-lodging monitoring in other areas, especially for cloudy and rainy regions where optical remote-sensing data are limited.

Author Contributions: Conceptualization, S.C.; methodology, X.D.; software, H.J.; validation, X.D.; formal analysis, K.J. and D.L.; investigation, Y.S.; resources, S.C.; writing—original draft preparation, X.D.; writing—review and editing, X.D.; visualization, K.J.; supervision, J.H.; project administration, S.C.; funding acquisition, S.C., Q.Z. and H.J. All authors have read and agreed to the published version of the manuscript.

Funding: This research was funded by Guangdong Province Agricultural Science and Technology Innovation and Promotion Project (No. 2022KJ102, No. 2023KJ102), GDAS Project of Science and Technology Development (2022GDASZH-2022010102, 2022GDASZH-2022010202), The National Natural Science Foundation of China (No. 42071417), Guangzhou Basic and Applied Basic Research Foundation (202102020691).

Data Availability Statement: Publicly available datasets were analyzed in this study. Sentinel-1 and Sentinel-2 data can be found here: [ESA, <https://scihub.copernicus.eu/dhus/#/home> (accessed on 20 December 2022)]. Gaofen-6 data can be found here: [CCRSD, <http://218.247.138.119:7777/DSSPlatform/index.html> (accessed on 20 December 2022)]. The website registration is open and free to the public.

Acknowledgments: We are very grateful to the reviewers for their constructive comments who significantly contributed to the improvement of this paper.

Conflicts of Interest: The authors declare no conflict of interest.

Appendix A

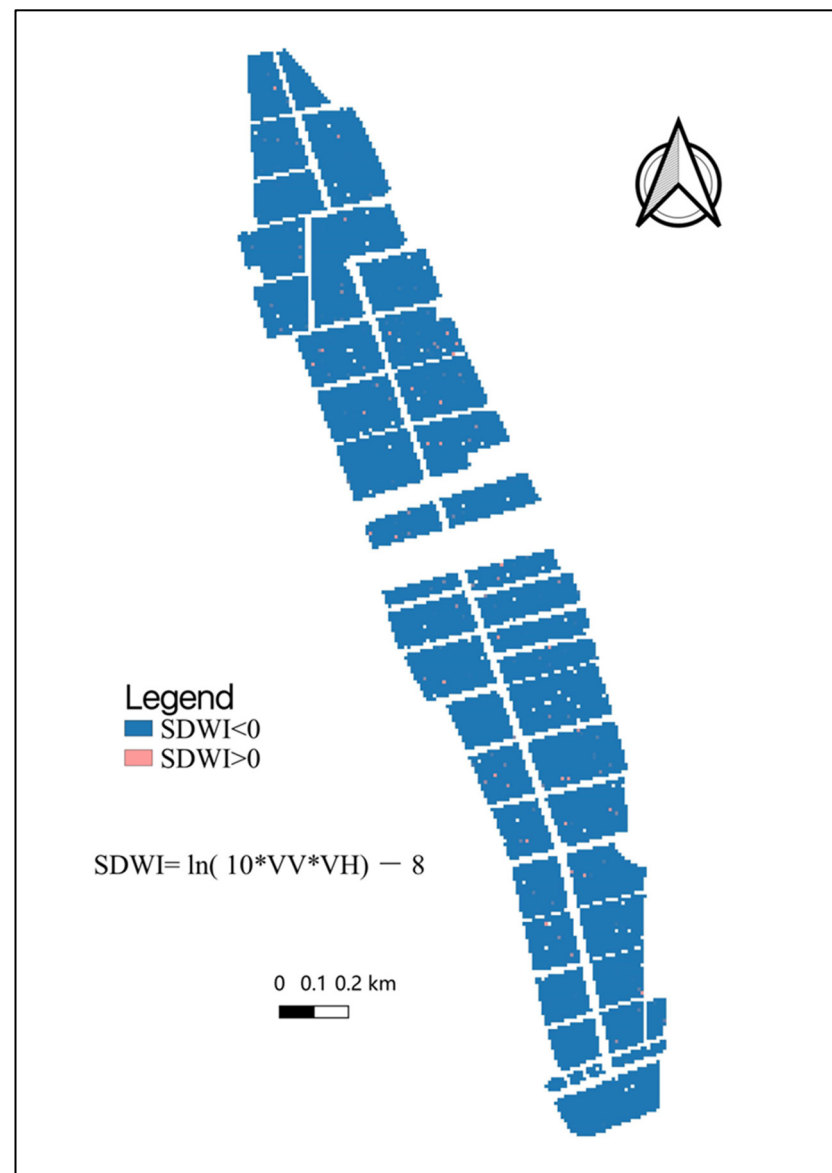


Figure A1. Dual-Polarized Water Index(SDWI) result.

References

- Kahan, D. The State of Food and Agriculture Innovation in Family Farming. Justice of China. 2014. Available online: https://www.researchgate.net/publication/269762372_The_State_of_Food_and_Agriculture_Innovation_in_family_farming (accessed on 6 June 2014).
- Zhou, P.; Zhou, K.; Liu, T.; Wu, W.; Sun, C. Progress in monitoring research on rice lodging. *J. Chin. Agric. Mech.* **2019**, *40*, 162–168. [CrossRef]
- Chauhan, S.; Darvishzadeh, R.; Boschetti, M.; Pepe, M.; Nelson, A. Remote sensing-based crop lodging assessment: Current status and perspectives. *ISPRS J. Photogramm. Remote Sens.* **2019**, *151*, 124–140. [CrossRef]
- Zhao, X.; Yuan, Y.; Song, M.; Ding, Y.; Lin, F.; Liang, D.; Zhang, D. Use of unmanned aerial vehicle imagery and deep learning unet to extract rice lodging. *Sensors* **2019**, *19*, 3859. [CrossRef] [PubMed]
- Ajadi, O.A.; Liao, H.; Jaacks, J.; Delos Santos, A.; Kumpatla, S.P.; Patel, R.; Swatantran, A. Landscape-Scale Crop Lodging Assessment across Iowa and Illinois Using Synthetic Aperture Radar (SAR) Images. *Remote Sens.* **2020**, *12*, 3885. [CrossRef]
- Wu, W.; Wang, W.; Meadows, M.E.; Yao, X.; Peng, W. Cloud-based typhoon-derived paddy rice flooding and lodging detection using multi-temporal Sentinel-1&2. *Front. Earth Sci.* **2019**, *13*, 682–694. [CrossRef]
- Quiros Vargas, J.; Khot, L.R.; Peters, R.T.; Chandel, A.K.; Molaei, B. Low Orbiting Satellite and Small UAS-Based High-Resolution Imagery Data to Quantify Crop Lodging: A Case Study in Irrigated Spearmint. *IEEE Geosci. Remote Sens. Lett.* **2020**, *17*, 755–759. [CrossRef]
- Liu, T.; Li, R.; Zhong, X.; Jiang, M.; Jin, X.; Zhou, P.; Liu, S.; Sun, C.; Guo, W. Estimates of rice lodging using indices derived from UAV visible and thermal infrared images. *Agric. For. Meteorol.* **2018**, *252*, 144–154. [CrossRef]
- Su, Z.; Wang, Y.; Xu, Q.; Gao, R.; Kong, Q. LodgeNet: Improved rice lodging recognition using semantic segmentation of UAV high-resolution remote sensing images. *Comput. Electron. Agric.* **2022**, *196*, 106873. [CrossRef]
- Chauhan, S.; Darvishzadeh, R.; Lu, Y.; Stroppiana, D.; Boschetti, M.; Pepe, M.; Nelson, A. Wheat lodging assessment using multispectral UAV data. In Proceedings of the International Archives of the Photogrammetry, Remote Sensing and Spatial Information Sciences, Enschede, The Netherlands, 10–14 June 2019; Volume 13, pp. 235–240. [CrossRef]
- Zheng, E.; Tian, Y.; Chen, T. Region extraction of corn lodging in UAV images based on deep learning. *J. Henan Agric. Sci.* **2018**, *47*, 155–160. [CrossRef]
- Lu, Z.; Xu, F.; Luo, M.; Liang, S.; Zhao, C.; Feng, X. Characteristic analysis of lodging rice and study of the multi-spectral remote sensing extraction method. *Chin. J. Eco-Agric.* **2021**, *29*, 751–7614. [CrossRef]
- Xie, X.R.; Xiao-He, G.U.; Lin, L.Q.; Yang, G.J.; Zhang, L.Y. Analysis of effect and spectral response of lodging stress on the ratio of visible stem, leaf and panicle in rice. *Spectrosc. Spectr. Anal.* **2019**, *39*, 2264–2270. [CrossRef]
- Wang, J.; Li, K.; Shao, Y.; Zhang, F.; Wang, Z.; Guo, X.; Qin, Y.; Liu, X. Analysis of Combining SAR and Optical Optimal Parameters to Classify Typhoon-Invasion Lodged Rice: A Case Study Using the Random Forest Method. *Sensors* **2020**, *20*, 7346. [CrossRef] [PubMed]
- Guan, H.; Huang, J.; Li, X.; Zeng, Y.; Su, W.; Ma, Y.; Wang, W. An improved approach to estimating crop lodging percentage with Sentinel-2 imagery using machine learning. *Int. J. Appl. Earth Obs. Geoinf.* **2020**, *113*, 102992. [CrossRef]
- Yulong, B.; Jiquan, Z.; Xiaojing, L. Study and analysis of canopy reflection information of crops affected by wind disaster. *Spectrosc. Spectr. Anal.* **2013**, *33*, 1057–1060, (In Chinese with English abstract). [CrossRef]
- Shu, M.; Zhou, L.; Gu, X.; Ma, Y.; Sun, Q.; Yang, G.; Zhou, C. Monitoring of maize lodging using multi-temporal Sentinel-1 SAR data. *Adv. Space Res.* **2019**, *65*, 470–480. [CrossRef]
- Han, D.; Yang, H.; Yang, G.J.; Qiu, C. Monitoring model of maize lodging based on Sentinel-1 radar image. *Trans. Chin. Soc. Agric. Eng. (Trans. CSAE)* **2018**, *34*, 166–172, (In Chinese with English abstract). [CrossRef]
- Guan, H.; Huang, J.; Li, L.; Li, X.; Ma, Y.; Niu, Q.; Huang, H. A novel approach to estimate maize lodging area with PolSAR data. *IEEE Trans. Geosci. Remote Sens.* **2022**, *60*, 1–17. [CrossRef]
- Yang, H.; Chen, E.; Li, Z.; Zhao, C.; Yang, G.; Pignatti, S.; Casa, R.; Zhao, L. Wheat lodging monitoring using polarimetric index from RADARSAT-2 data. *Int. J. Appl. Earth Obs. Geoinf.* **2015**, *34*, 157–166. [CrossRef]
- Moldenhauer, K.E.W.C.; Slaton, N. Rice growth and development. *Rice Prod. Handb.* **2001**, *192*, 7–14.
- Nelson, A.; Setiyono, T.; Rala, A.B.; Quicho, E.D.; Raviz, J.V.; Abonete, P.J.; Maunahan, A.A.; Garcia, C.A.; Bhatti, H.Z.; Villano, L.S.; et al. Towards an operational SAR-based rice monitoring system in Asia: Examples from 13 demonstration sites across Asia in the RIICE project. *Remote Sens.* **2014**, *6*, 10773–10812. [CrossRef]
- Dey, S.; Bhogapurapu, N.; Homayouni, S.; Bhattacharya, A.; McNairn, H. Unsupervised Classification of Crop Growth Stages with Scattering Parameters from Dual-Pol Sentinel-1 SAR Data. *Remote Sens.* **2021**, *13*, 21. [CrossRef]
- Li, Z.C.; Li, Y.H.; Zhou, H.M. Monitoring of paddy rice crop with remote sensing technology based on multi-temporal dual polarization ALOS-PALSAR images—A case study of Deyang county. *J. Southwest China Norm. Univ. (Nat. Sci. Ed.)* **2012**, *41*, 393–410. [CrossRef]
- Multi-temporal and dual-polarimetric TerraSAR-X data. *Int. J. Appl. Earth Obs. Geoinf.* **2013**, *21*, 568–576. [CrossRef]
- Zhao, L.; Yang, J.; Li, P.; Shi, L.; Zhang, L. Characterizing lodging damage in wheat and canola using Radarsat-2 polarimetric SAR data. *Remote Sens. Lett.* **2017**, *8*, 667–675. [CrossRef]
- Cloude, S.R.; Pottier, E. An entropy based classification scheme for land applications of polarimetric SAR. *IEEE Trans. Geosci. Remote Sens.* **1997**, *35*, 68–78. [CrossRef]

28. Story, M.; Congalton, R.G. Accuracy assessment: A user's perspective. *Photogramm. Eng. Remote Sens.* **1986**, *52*, 397–399.
29. Zhu, C.; Luo, J.; Shen, Z.; Cheng, X. Winter wheat planting area extraction using multi-temporal remote sensing images based on field parcel. *Trans. Chin. Soc. Agric. Eng. (Trans. CSAE)* **2018**, *34*, 157–164. (In Chinese with English abstract) [[CrossRef](#)]
30. Breiman, L. Random Forests. *Mach. Learn.* **2001**, *45*, 5–32. [[CrossRef](#)]
31. Lengauer, T. Permutation importance: A corrected feature importance measure. *Bioinformatics* **2010**, *26*, 1340–1347. [[CrossRef](#)]
32. Chauhan, S.; Darvishzadeh, R.; Lu, Y.; Boschetti, M.; Nelson, A. Understanding wheat lodging using multi-temporal Sentinel-1 and Sentinel-2 data. *Remote Sens. Environ.* **2020**, *243*, 111804. [[CrossRef](#)]
33. Chauhan, S.; Darvishzadeh, R.; Boschetti, M.; Nelson, A. Discriminant analysis for lodging severity classification in wheat using RADARSAT-2 and Sentinel-1 data. *557 ISPRS J. Photogramm. Remote Sens.* **2020**, *164*, 138–151. [[CrossRef](#)]
34. Wang, L.F.; Kong, J.A.; Ding, K.H.; Le Toan, T.; Ribbes, F.; Floury, N. Electromagnetic scattering model for rice canopy based on Monte Carlo simulation. *Prog. Electromagn. Res.* **2005**, *52*, 153–171. [[CrossRef](#)]
35. Wang, H.; Magagi, R.; Gouita, K.; Trudel, M.; McNairn, H.; Powers, J. Crop phenology retrieval via polarimetric SAR decomposition and random Forest algorithm. *Remote Sens. Environ.* **2019**, *231*, 111234. [[CrossRef](#)]
36. Chauhan, S.; Srivastava, H.S.; Patel, P. Wheat crop biophysical parameters retrieval using hybrid-polarized RISAT-1 SAR data. *573 Remote Sens. Environ.* **2018**, *216*, 28–43. [[CrossRef](#)]
37. McNairn, H.; Brisco, B. The application of C-band polarimetric SAR for agriculture: A review. *Can. J. Remote Sens.* **2004**, *30*, 525–542. [[CrossRef](#)]
38. Niu, L.; Feng, S.; Ding, W.; Li, G. Influence of speed and rainfall on large-scale wheat lodging from 2007 to 2014 in China. *PloS ONE* **2016**, *11*, e0157677. [[CrossRef](#)]
39. Huang, Z.; Wang, H.; Chen, X. Characteristics of “dragon boat water” and its impact on the early rice yield under climate change. *Ecol. Environ. Sci.* **2011**, *20*, 793–797. [[CrossRef](#)]
40. Zhang, Z.; Flores, P.; Igathinathane, C.; LNaik, D.; Kiran, R.; Ransom, J.K. Wheat Lodging Detection from UAS Imagery Using Machine Learning Algorithms. *Remote Sens.* **2020**, *12*, 1838. [[CrossRef](#)]
41. Jiang, B. Comparison of Inversion Results on Water Color Remote Sensing Based on Traditional Empirical Models and Machine Learning Models. Master's Thesis, University of Chinese Academy of Sciences, Beijing, China, 2021.
42. Chauhan, S.; Darvishzadeh, R.; van Delden, S.H.; Boschetti, M.; Nelson, A. Mapping of wheat lodging susceptibility with synthetic aperture radar data. *Remote Sens. Environ.* **2021**, *259*, 112427. [[CrossRef](#)]
43. Qian, L.; Jiang, H.; Chen, S.; Li, D.; Wang, C.; Chen, J.; Dai, X. Extracting field-scale crop distribution in Lingnan using spatiotemporal filtering of Sentinel-1 time-series data. *Trans. Chin. Soc. Agric. Eng. (Trans. CSAE)* **2022**, *38*, 158–166. (In Chinese with English abstract) [[CrossRef](#)]

Disclaimer/Publisher's Note: The statements, opinions and data contained in all publications are solely those of the individual author(s) and contributor(s) and not of MDPI and/or the editor(s). MDPI and/or the editor(s) disclaim responsibility for any injury to people or property resulting from any ideas, methods, instructions or products referred to in the content.